

## The Impact of Solution Agglomeration on the Deposition of Self-Assembled Monolayers

Bruce C. Bunker, Robert W. Carpick\*, Roger Assink, Mike Thomas, Matt Hankins, Jim Voigt, Diana Sipola, Martin DeBoer, and Gerald Gulley  
Sandia National Laboratories, Albuquerque, NM 87185

\* present address: Engineering Physics Department, University of Wisconsin - Madison, 1500 Engineering Dr., Madison, WI 53706-1687.

RECEIVED  
MAY 04 2000  
OSTI

### Abstract

Self-assembled monolayers (SAMS) are commonly produced by immersing substrates in organic solutions containing trichlorosilane coupling agents. Unfortunately, such deposition solutions can also form alternate structures including inverse micelles and lamellar phases. The formation of alternate phases is one reason for the sensitivity of SAM depositions to factors such as the water content of the deposition solvent. If such phases are present, the performance of thin films used for applications such as minimization of friction and stiction in micromachines can be seriously compromised. Inverse micelle formation has been studied in detail for depositions involving 1H-, 1H-, 2H-, 2H- perfluorodecyltrichlorosilane (FDTS) in isooctane. Nuclear magnetic resonance experiments have been used to monitor the kinetics of hydrolysis and condensation reactions between water and FDTS. Light scattering experiments show that when hydrolyzed FDTS concentrations reach a critical concentration, there is a burst of nucleation to form high concentrations of spherical agglomerates. Atomic force

## **DISCLAIMER**

**This report was prepared as an account of work sponsored by an agency of the United States Government. Neither the United States Government nor any agency thereof, nor any of their employees, make any warranty, express or implied, or assumes any legal liability or responsibility for the accuracy, completeness, or usefulness of any information, apparatus, product, or process disclosed, or represents that its use would not infringe privately owned rights. Reference herein to any specific commercial product, process, or service by trade name, trademark, manufacturer, or otherwise does not necessarily constitute or imply its endorsement, recommendation, or favoring by the United States Government or any agency thereof. The views and opinions of authors expressed herein do not necessarily state or reflect those of the United States Government or any agency thereof.**

## **DISCLAIMER**

**Portions of this document may be illegible in electronic image products. Images are produced from the best available original document.**

microscopy results show that the agglomerates then deposit on substrate surfaces. Deposition conditions leading to monolayer formation involve using deposition times that are short relative to the induction time for agglomeration. After deposition, inverse micelles can be converted into lamellar or monolayer structures with appropriate heat treatments if surface concentrations are relatively low.

## **Introduction**

Self-assembled monolayers (SAMS) formed using organosilane coupling agents are used extensively to modify the fundamental properties of surfaces for a wide range of technological applications. For example, such coupling agents provide one method for attaching hydrocarbon or fluorocarbon chains to silicon wafers to control friction and stiction in micromachines.<sup>1</sup> Unfortunately, coating processes involving silanes are known to be highly irreproducible, and film properties such as water contact angle can be highly variable.<sup>2</sup> Factors known to influence depositions include temperature<sup>3</sup>, the solvent and its water content<sup>4</sup>, coupling agent concentrations, surface preparation<sup>5</sup>, and even what container the substrates are coated in. Once layers are deposited, coating properties can continue to change. For example, exposures of SAMS to humid air can gradually degrade the hydrophobic character of the film, leading to increased adhesion with time.<sup>6</sup>

All of the above phenomena are influenced by the extent to which molecules of coupling agents interact with each other both in solution and on the substrate surface. In the classical description of assembly on a surface<sup>7</sup>, chlorosilane coupling agents are assumed to have a low affinity for the surface until they react with water to form

hydroxysilanes (Fig. 1). The –OH groups in the hydroxysilanes can hydrogen bond to each other and to surface hydroxyl groups. Interactions between the hydrocarbon chains direct chain ordering to form a dense monolayer. Finally, a condensation reaction is assumed to occur in which hydroxyl groups react with each other to form Si-O-Si linkages within the monolayer and to the surface. The net result of the above sequence would be the production of a dense, robust film that is highly crosslinked both laterally and to the Si substrate.

While simple and compelling, the above picture glosses over several features of silane deposition processes that can lead to irreproducible results. First, deposition models tend to focus on hydrolysis and condensation on the substrate surface while ignoring the fact that the same reactions also occur in solution. If hydrolyzed molecules of the coupling agent form hydrogen bonded (and eventually siloxane bonded) networks on a surface, it is likely that such networks also form in solution as in the so-called “sol-gel” processing of silica.<sup>8</sup> The fact that coupling agent solutions become cloudy with time shows that such aggregation does indeed occur. It is likely that the aggregation is not a random process, but involves self-assembly phenomena to form micelles or other extended structures (e.g. lamellar, hexagonal, and cubic phases) similar to those observed for common oil-water-surfactant systems.<sup>25</sup> If these aggregates assemble and interact with the surface during film formation, monolayers will not be produced unless surface interactions are strong enough to restructure the aggregates.

A related problem is that even if monolayers are initially produced, it is possible that surface structures can rearrange to form alternate phases in response to changing environmental conditions unless cross-linking within the film is pronounced. Although

NMR results for high surface area materials suggest that condensation can be extensive<sup>9</sup>, other researchers report that the extent of condensation is negligible<sup>10</sup>. Recent results on reversible phase changes in films of octadecyltrichlorosilane (ODTS) spread on a thin water layer on silicon substrates suggest that the extent of condensation, even between adjacent molecules, is relatively low<sup>11</sup>. Individual molecules within the SAM appear to be mobile, indicating that head group interactions involve hydrogen bonding rather than formation of covalent bonds. Molecular mobility may be critical during film formation, but could lead to serious problems with regard to long-term film stability if condensation reactions do not lock the films into place before they have a chance to rearrange.

The purpose of this investigation is to examine structures produced in solution and on substrate surfaces for a specific thin film deposition system consisting of 1H-, 1H-, 2H-, 2H- perfluorodecyltrichlorosilane (FDTS) dissolved in isooctane. The hydrocarbon chain of FTDS has ten carbons of which all but the two adjacent to the -SiCl<sub>3</sub> group are fluorinated to make the chains more hydrophobic. Such fluorocarbon chains are reported to have antistiction and antifricition properties superior to those exhibited by hydrocarbon chains.<sup>12</sup> Isooctane was investigated as the solvent to address environmental concerns (against aromatic and chlorinated solvents). Although effective antistiction coatings have been produced using FTDS-isooctane solutions, the existing coating process is known to be even harder to control than ODTS depositions. Goals of the work are to identify mechanisms for the development of film structures and guidelines for selecting optimum processing conditions for fabricating high-quality films.

The focus of this work involves identifying mechanisms for the development of film structures and guidelines for optimizing film processing conditions. The primary

processing variables of interest involve the deposition solution. First, it is widely recognized that control of the water content is critical to the formation of dense silane monolayers. Higher water contents are expected to accelerate the rate of coupling agent hydrolysis both in solution and on the surface. However, how much water is required for optimum films is open to debate. Some groups claim that discrete layers of water must be present on the immediate silica surface for SAMS to form<sup>5</sup>, while other groups claim<sup>4</sup> that water in the bulk solvent is required to get good films. The amount of water required for complete hydrolysis of a trichlorosilane is three times the moles of silane present (3 mM for a standard 1 mM silane deposition solution). However, such high water contents could promote rapid hydrolysis and condensation in solution, precipitating the coupling agent before it has a chance to react with the surface. At the other extreme, the quantity of water required for hydrolysis of a complete self-assembled monolayer on silica (around 5 silane molecules per nm<sup>2</sup>) is 7.5 water molecules/nm<sup>2</sup>. (as little as  $2 \times 10^{-7}$  M if initially dissolved in the solvent). However, maintaining water layers on the silica surface probably requires that the solvent be near or above the water saturation limit (otherwise the surface water will dissolve into the solvent). For isooctane, the saturation water content is  $2.3 \times 10^{-3}$  M, which is similar to the concentration required for complete hydrolysis of the dissolved silanes. Some researchers claim<sup>4</sup> that the best films are achieved at intermediate concentrations ( $1 \times 10^{-4}$  M, or sufficient water to completely react with 7% of the chlorosilane molecules present).

A second critical variable in coating solutions is the deposition solvent. The solvent system plays a major role in controlling the solubility and reactivity of both water and the coupling agent. The solubility limits for water in the primary solvents

investigated in this study are 2.5 mM, 8 mM, and 60 mM for isooctane,  $\text{CCl}_4$ , and  $\text{CHCl}_3$ , respectively. The same solvation effects that increase the water solubility are also expected to enhance the “solubility” of Si-OH groups in the hydrolyzed head group, suppress the “solubility” of the fluorocarbon tails, and thus influence the stability regimes of phases in the surfactant-solvent-water phase diagram. The distribution of water between the solution and the substrate surface is also influenced by the solvent. At a water content of  $2.5 \times 10^{-3}$  M, the driving force for water to leave isooctane and form either surface layers on substrates or solution aggregates such as inverse micelles should be much greater than it is in  $\text{CHCl}_3$ . Conversely, water layers present on Si prior to processing would be expected to dissolve in a  $2.5 \times 10^{-3}$  M solution of water in  $\text{CHCl}_3$ . If the best coatings are produced with the maximum surface water and the minimum bulk water concentrations (insuring that hydrolysis is favored on the substrate rather than in solution), then isooctane should be the most effective solvent of the three in promoting monolayer formation. Finally, more polar solvents such as chloroform ( $\text{CHCl}_3$ ) are expected to promote the kinetics of hydrolysis and condensation by stabilizing the polar intermediates involved in nucleophilic attack on tetrahedral Si centers. At identical water contents, reaction rates in  $\text{CHCl}_3$  are expected to be more rapid than those in isooctane.

The role of water and the solvent in mediating film formation have been determined using a range of techniques that probe what is happening to the coupling agent both in solution and the substrate surface. The kinetics of hydrolysis and condensation of FDTS in the solution phase have been determined using  $^{17}\text{O}$  nuclear magnetic resonance (NMR) techniques to follow the solution concentrations of water and oxygen-containing products. Light scattering methods have been used to determine



whether such hydrolysis and condensation leads to the formation of FDTS aggregates in solution. In parallel, contact angle and ellipsometry measurements have been used to determine the kinetics of film formation on Si substrates, while atomic force microscopy (AFM) has been used to image thin film structures. The above combination of techniques has enabled us to identify the critical solution parameters that influence the processing, structures, and performance of FTDS thin films. The results show that solution aggregates can be incorporated into film structures, contributing to irreproducible film properties.

## **Experimental Section**

Reagent grade solvents including isooctane, chloroform, and carbon tetrachloride were utilized without further purification. Solvent water content was varied by saturating quantities of each solvent via equilibration with a layer of water or by drying with activated molecular sieves (4A zeolites). Intermediate water contents were obtained by mixing appropriate quantities of the wet and dry solvents. The water content of each solvent used was measured using a Karl Fisher titration system (Accumet KF Titrator 150, Fisher Scientific). The 1H-, 1H-, 2-H, 2H- perfluorodecyltrichlorosilane (Lancaster) was used without further purification. All FDTS was stored in a dry box prior to use. Additions of FTDS to solvents for either solution hydrolysis or Si wafer coating experiments were performed in a dry box.

$^{17}\text{O}$  NMR spectra were obtained on a Bruker AMX-400 spectrometer operating at 54.3 MHz using a 5 mm probe. A Hahn spin-echo pulse sequence was used in order to reduce baseline distortions. The spectra were recorded with a  $90^\circ$  pulse width of 20

msec, a spin-echo time of 10 msec, and a 100 ms repetition delay. The number of scans varied from 1000-4000. All spectra were externally referenced to  $\text{H}_2^{17}\text{O}$  (0 ppm). In a typical NMR experiment,  $\text{H}_2^{17}\text{O}$  (20%  $^{17}\text{O}$  enriched water from Isotec Inc.) was equilibrated with the desired solvent at the desired concentration for up to one day. At  $t = 0$ , the desired concentration (typically 1 mM) of coupling agent was added to the solution in the NMR tube and rapidly mixed prior to introduction into the spectrometer. Spectra were collected at regular time intervals for periods up to several days. All oxygen-containing species could be detected down to concentrations of around  $10^{-4}$  M.

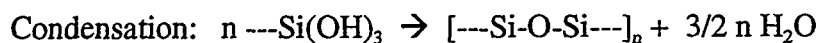
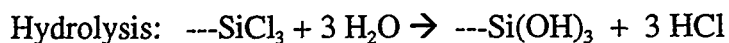
The average radius of gyration of objects dispersed in the solution was obtained using quasielastic light scattering (QELS) equipment and analysis methods described previously.<sup>13</sup> In the quasi-elastic light-scattering experiments, the intensity  $I(q)$  of light scattered at wave vector  $q$  was autocorrelated to obtain the homodyne correlation function  $C(t) = \langle I(q,0)I(q,t) \rangle$ . The dynamic structure factor  $S(q,t)$  was obtained from the standard relation  $S(q,t) = [C(t) - \langle I(q,0)I(q, \infty) \rangle]^{1/2}$ . The data were analyzed assuming the solutions contain monodisperse spheres for which the structure factor is given by  $S(q,t) = S(q)\exp(-q^2Dt)$  where  $S(q)$  is the static structure factor,  $D = kT/6\pi\eta R$  is the translational diffusion coefficient, and  $R$  is hydrodynamic radius. Data are presented in terms of the hydrodynamic radius, which (for spheres) is equal to  $R_g/0.775$  where  $R_g$  is the radius of gyration. In a typical experiment, FDTS was added to the isooctane, quickly stirred, added to a syringe equipped with a  $0.2 \mu\text{m}$  filter to remove particulates, and injected into 50 ml quartz cuvettes that were then inserted into the light scattering system. Scattered light intensity was typically collected at an angle of  $90^\circ$  to the incident laser beam as a function of time

Silicon wafers were cut into 1 cm x 1 cm squares. Prior to exposure to coating solutions, the wafers were cleaned using standard Piranha etching solutions to remove organic contaminants. In a typical coating experiment, 37  $\mu\text{l}$  of FDTS was added to 50 ml of solvent to make a 1 mM FDTS solution. Solutions were quickly stirred, and the Si square was immediately dipped into the solution for a specific time interval (ranging from ten minutes to over two hours). Samples were removed from the coating solution, rinsed in plain solvent to remove excess coupling agent, and dried in the box. Some samples were then heat treated in a low temperature oven or in a rapid thermal processing unit (AET Model Addax R4M) at temperatures of from 150°C to 400°C and times ranging from 30 seconds to five minutes. Coating thicknesses were estimated using an ellipsometer (J. A. Woollam Co. Model WVASE32). Contact angle measurements were performed using a static droplet video contact angle system (Advanced Surface Technology, Inc. Model VCA 2500). Atomic force microscopy (AFM) topography measurements were obtained using a Digital Instruments Nanoscope IIIA in both tapping and contact modes.

## **Results**

### **<sup>17</sup>O NMR Results - Kinetics of Hydrolysis and Condensation in Solution**

To determine the optimum reaction conditions for attaching silane coupling agents to surfaces, information is required regarding how fast water reacts with the coupling agent to produce active species. The hydrolysis and condensation reactions relevant to activating and consuming trichlorosilane coupling agents in water are:



Nuclear magnetic resonance techniques can be used to monitor the concentrations of the reactants and products involved in both hydrolysis and condensation reactions in solution as a function of time. NMR-active nuclei that could be used in following reaction kinetics include  $^{29}\text{Si}$ ,<sup>14</sup> H, D,  $^{17}\text{O}$ ,<sup>8</sup> and (for FDTS)  $^{19}\text{F}$ .<sup>15</sup> In this investigation,  $^{17}\text{O}$  NMR was utilized for the bulk of the experiments. All  $^{17}\text{O}$  present in the initial solution is in the form of  $\text{H}_2^{17}\text{O}$ , which has a sharp resonance at around 0 ppm. As the water reacts with the coupling agent, new NMR peaks can be observed associated with Si-OH (near 25 ppm) and Si-O-Si (from 50-70 ppm). The rate at which the water signal disappears is used to determine the kinetics of hydrolysis, while the rate of appearance of the Si-O-Si peak can be used to establish the kinetics of condensation.

$^{17}\text{O}$  NMR results have been obtained for water contents and coupling agent concentrations both ranging from 1- 8 mM in isooctane and carbon tetrachloride. Representative NMR spectra in  $\text{CCl}_4$  and isooctane (Fig. 2) show that at short times the water concentration decreases and the Si-OH concentration increases consistent with hydrolysis of the coupling agent (Fig. 3). As expected, the initial hydrolysis rate increases with the initial FDTS and water concentrations. The specific rate law has not been determined, as the HCl liberated in the reaction (e.g. pH) is known to influence the reaction kinetics. However, for a 1 mM solution of FDTS in water saturated (2.3 mM) isooctane, the first reaction stage has a pseudo first order rate constant of  $3 \times 10^{-3} \text{ min}^{-1}$

(would be 50% complete in 90 minutes). At longer times, the Si-OH peak disappears, and the rate of water consumption is ten times slower (pseudo first order rate constant of  $4 \times 10^{-4} \text{ min}^{-1}$ ). The maximum Si-OH concentration reached in isooctane is around 0.6 mM (20% of the available FDTS, which has three equivalents of Si-Cl bonds per molecule for a total of 3 mM). This maximum concentration is reached at fairly short reaction times (15-20 minutes for a 1 mM FDTS + 2.3 mM H<sub>2</sub>O solution in isooctane). For more concentrated solutions (8 mM in both FDTS and water) in CCl<sub>4</sub>, the peak Si-OH concentration is higher (2.3 mM) and is reached more quickly (in 4 minutes) than in the more dilute isooctane solution (Fig. 3b). However, no new NMR peaks are observed corresponding to the formation of Si-O-Si linkages in either isooctane or CCl<sub>4</sub>. Instead, there is a decrease in the total <sup>17</sup>O NMR signal. The decrease (an 80% drop in 6 hours for FDTS in CCl<sub>4</sub>) is much more than can be accounted for on the basis of the formation of a monolayer of FTDS on the walls of the NMR tube (which would account for a loss of 0.3%). The loss in intensity either means that films containing hundreds of FDTS layers are being deposited or that objects are being formed in solution that are sufficiently large to broaden the NMR signals associated with them into the baseline.

The only solution investigated in which NMR spectra indicate the formation of Si-O-Si bonds has high concentrations ( $1.7 \times 10^{-2} \text{ M}$ ) of both water and FDTS in the polar solvent chloroform (CHCl<sub>3</sub>) (Fig. 4). In this solution, the rate constant for water consumption is one hundred times greater than that seen in dilute isooctane (85% gone in 7 minutes for a pseudo first order rate constant of around  $0.3 \text{ min}^{-1}$ ). However, in addition to the Si-OH signal near 25 ppm, significant NMR intensity is also observed at around 50 ppm indicative of the formation of FTDS dimers (one bridging oxygen). At

longer times, a broad series of peaks appears in the 50-75 ppm regime indicative of soluble species containing two and even three Si-O-Si linkages per molecule. In potassium silicate solutions, such NMR peaks have been attributed to soluble species such as cyclic trimers and tetramers and prismatic hexamers.<sup>16</sup> For FDTS, small cages are expected as reported for silsequioxane solutions.<sup>17</sup> Condensation is probably promoted in CHCl<sub>3</sub> and not in isooctane or CCl<sub>4</sub> due to the increased polarity of CHCl<sub>3</sub>, which promotes reactions involving nucleophilic attack. At longer times, the Si-OH peak does not drop toward zero. The constant value of  $8 \times 10^{-3}$  M reached for the Si-OH concentration from hydrolyzed FDTS monomers may represent the solubility limit in CHCl<sub>3</sub>. However, as seen in isooctane and CCl<sub>4</sub>, the total observable <sup>17</sup>O signal decreases with time (70% is gone in 7 minutes) indicative of the formation of large objects in solution or multilayer depositions.

#### Light Scattering Results – Particle Dimensions and Kinetics of Particle Formation

While the NMR results provide information regarding the total fraction of FDTS that disappears from coating solutions, no information is provided regarding the nature of the missing material. We used light scattering methods<sup>18</sup> to determine if precipitates or micelles form and to obtain estimates of the average hydrodynamic radius and relative concentration of objects in isooctane coating solutions as a function of time. Immediately after FDTS addition, light scattering from the solutions is negligible (Fig. 5a), indicating that foreign particles are not present at appreciable concentrations. For a 1 mM FDTS solution in isooctane containing 0.75 mM water, scattering continues to be low for 10 to 20 minutes after mixing. Then, there is a sudden burst of nucleation. While induction

times are variable (as expected for a nucleation process), they are comparable to the times at which Si-OH concentrations begin to drop in the  $^{17}\text{O}$  NMR experiments. The first objects observed have a hydrodynamic radius of 75 nm (Fig. 5b). These objects grow and stabilize at a radius of 130 nm over the next 10-15 minutes. The relative concentration of the objects as inferred from the total scattered intensity increases by a factor of ten during this period. Objects continue to form even after further particle growth is negligible, consistent with the slow but continued hydrolysis indicated in the NMR experiments. Visual inspection of the solution in the cuvette indicates that the distribution of particles within the static solutions can be highly variable. Sometimes, objects appear to nucleate within the center of the cuvette, while in other experiments, nucleation starts near the walls. Sometimes, “banded” structures are observed which move in the cuvette with time. Such effects contribute to the observed scatter in both induction times and total scattered intensity as a function of time.

The induction time for nucleation decreases as the initial water content of the isooctane increases. The sensitivity of the induction time to water content is one reason for the irreproducible behavior of FDTS coating solutions. The rate at which particles are produced also increases with water content. For 1 mM FDTS solutions in isooctane, the time required for the scattered intensity to saturate the detector (at  $10^6$  counts) decreases from 130 minutes to 25 minutes to 10 minutes as the initial water content is increased from 0.2 mM to 0.8 mM to 4.3 mM, respectively. Finally, the stable radius for the particles increases with water content from 95 nm to 130 nm to almost 800 nm for the solutions mentioned above. All of these particles are large relative to the chain length of individual FDTS molecules (1.5 nm).

## Contact Angle Measurements - Deposition Rates for FDTS Films

Contact angle measurements involving sessile drops of deionized water have been used to follow the kinetics of film formation on Si wafers immersed in FDTS solutions having similar compositions to those used in the NMR experiments. Water exhibits a relatively low contact angle (around 30°) on normal Si due to hydrogen bonding between the water and the silanols which terminate the surface of the thermal oxide. As hydrophobic coupling agents are deposited on the surface, the contact angle increases with time. For a complete monolayer, the expected contact angle can be calculated using the Young equation:<sup>19</sup>

$$\gamma_{12} + \gamma_2 \cos \theta = \gamma_1$$

Calculated values for the contact angle of a complete monolayer are 110° and 115° for hydrocarbon and fluorocarbon SAMs, respectively. (Calculations are based on published values<sup>19</sup> for the surface tension of water ( $\gamma_2 = 73 \text{ mJ/m}^2$ ), the surface energy of the monolayer ( $\gamma_1 = 25 \text{ mJ/m}^2$  and  $19 \text{ mJ/m}^2$  for hydrocarbon and fluorocarbon chains, respectively), and the SAM-water interfacial energy ( $\gamma_{12} = 50 \text{ mJ/m}^2$  for both hydrocarbons and fluorocarbons).) For surfaces that are partially covered by domains of coupling agents, the surface coverage can be inferred using the Cassie equation:<sup>20</sup>

$$\cos \theta = f_1 \cos \theta_1 + f_2 \cos \theta_2$$



where  $f_1$  is the fractional area of the surface covered by the monolayer,  $f_2$  represents the uncovered surface, and  $\theta_1$  and  $\theta_2$  represent the contact angles for “pure” monolayer and uncovered surfaces (see Ref. 20 for a more rigorous treatment of contact angles on two component surfaces).

Typical contact angle results for Si substrates immersed in 1 mM solutions of FDTS in isooctane and  $\text{CCl}_4$  are shown in Fig. 6. Deposition kinetics mirror the kinetics of FDTS hydrolysis in solution. For isooctane solutions containing isopropanol (a solvent used in the part release cycle), no FDTS coatings are produced. This is because alcohols react with Si-Cl bonds to form Si-OR groups that interfere with Si-OH and monolayer formation. For all other solutions, the contact angle and inferred FDTS coverage increase rapidly at first. The deposition rate increases with solvent water content. Once contact angles approach those expected for the completed monolayer ( $115^\circ$ ), the contact angle continues to increase, but at a much slower rate. Times required to reach contact angles of  $115^\circ$  are comparable to those required to achieve the maximum Si-OH concentration in solution (two hours, 30 minutes, and less than seven minutes for 0.17 mM  $\text{H}_2\text{O}$  in isooctane, 2.3 mM  $\text{H}_2\text{O}$  in isooctane, and 2.3 mM  $\text{H}_2\text{O}$  in  $\text{CCl}_4$ , respectively.).

For most coating solutions, the observed contact angle continues to increase to values approaching  $120^\circ$ . In some instances, contact angles as high as  $140^\circ$  have been observed. Contact angles in excess of  $115^\circ$  are not indicative of continued packing of FTDS into the monolayer, but are associated with a roughening of the surface (see AFM results below). The ratio ( $r$ ) of the actual surface area relative to the geometric surface area can be estimated using the modified Young’s equation:<sup>21</sup>

$$\cos \theta_r = r \cos \theta$$

where  $\theta_r$  is the apparent contact angle and  $\theta$  is the inherent contact angle for the material at the surface ( $\theta = 115^\circ$  for FTDS). Based on a contact angle of  $140^\circ$ , the surface area increases by as much as a factor of around 1.8. Such increases in surface roughness are only apparent at times exceeding the nucleation time for formation of objects in solution as seen via light scattering.

#### Atomic Force Microscopy – Morphologies of FTDS Coatings on Silicon Substrates

We used atomic force microscopy (AFM) to determine if the roughening of the surface indicated by contact angle measurements is related to the adsorption of the objects detected in solution via light scattering. For the AFM studies, silicon substrates were immersed in FDTS coating solutions for specific times after mixing and were examined after drying in air. Samples immersed for short times in fresh FDTS solutions exhibited surface morphologies that were identical to uncoated Si substrates (flat regions in Fig. 7a). Although no coating is visible, ellipsometry measurements indicate that FDTS is being deposited during this initial coating stage. However, the apparent thickness of the coating stabilizes at 0.3-0.5 nm rather than at the 1.5 nm expected for a well organized FDTS coating having the fluorocarbon chains tightly packed and oriented perpendicular to the surface. The ellipsometry results are consistent with the deposition of chains in an “amorphous” phase in which the chains are lying flat on the surface with random orientations and with lower packing densities than found in a well organized self-

assembled monolayer.<sup>22</sup> For hydrocarbon chains, such films are typically observed when the hydrocarbon chain length is less than ten (FDTS has 10 carbons in the chain) or when deposition temperatures are above the transition temperature for ordering. Based on the rough correlation between melting point and transition temperature for ordering for hydrocarbon chains<sup>23</sup>, it is estimated that the ordering temperature for FDTS should be between 25°C-30°C. Although variable temperature studies were not conducted, it is likely that ordered monolayers can be produced from colder deposition solutions.

At times that roughly correspond to the induction times for nucleation of objects in solution, the surface morphology of the FDTS coatings undergoes a dramatic change (Fig. 7a). Tapping mode images show that FDTS is now present in the form of large circular objects. The diameter of the objects is normally slightly larger than twice the hydrodynamic radius of objects observed in the coating solution via light scattering. (For example, for isooctane solutions containing objects with a hydrodynamic radius of 130 nm, the diameter of the circular objects on the surface is around 300 nm.) Although these objects will subsequently be referred to as FDTS spheres, the objects are not spherical once deposited on a surface. AFM scans of the 300 nm diameter objects indicate a maximum thickness of around 25 nm (Fig. 7b). Therefore, the objects resemble liquid droplets that sag and “wet” the FDTS coated substrate. The number of droplets increases with time. In extreme cases, multilayers of the droplets have been observed, leading to film thicknesses in excess of 0.1  $\mu\text{m}$  as inferred by ellipsometry.

We have further probed the nature and stability of the FDTS by attempting to disturb the objects with the AFM tip (repeated scanning at high loads in contact mode) and by heating substrates coated with the spheres using rapid thermal processing (RTP)

techniques. Repeated AFM scanning of the same region at high loads does not move the spheres relative to the substrate. Instead, the moving tip gradually smears out the spheres in the scanning direction. The spheres behave like a viscous droplets containing mobile molecules rather than as rigid crosslinked solids.

When less than a monolayer of the spheres is present, heating the surface at 150°C for less than one minute is sufficient to completely change the surface morphology (Fig. 8a). Such a heat treatment would be sufficient to vaporize isooctane and water from the surface (isooctane has a boiling point of 99°C similar to water). Now the surface is partially covered by multilayered structures rather than spheres. Each layer is atomically flat, with a layer thickness corresponding to the length of the FDTS chains (1.8 nm)(Fig. 8b). The multilayer domains are not spherical, but are irregularly shaped, often with straight side edges. Most commonly, two layers are apparent, although three layers are sometimes observed.

Friction measurements, which require tip-sample contact, were difficult to obtain because of the soft character of the structures. However, we have obtained one set of data suggesting that there is a strong friction contrast between successive layers. The immediate surface alternates between sticky and non-sticky behavior, consistent with the classical lamellar structure seen for surfactants (Fig. 9). Such a structure has been reported previously for ODTS precipitates formed in water.<sup>24</sup> When the surface is terminated by fluorocarbon chains, tip-substrate interactions are weak and adhesion and friction are low, as expected for FDTS monolayers. However, every other layer is oriented with the chains pointing down and the Si-(OH)<sub>3</sub> groups pointing up. The silanol terminated surface is hydrophilic, can participate in extensive hydrogen bonding, and is

expected to be quite sticky. The AFM friction results indicate how sensitive the surface adhesion can be to the orientation and local structures assumed by the FDTs molecules.

FDTs coatings containing spheres (deposited from isooctane) have been heated at temperatures of 250°–400°C using rapid thermal processing. At 250°C, the films reorganize to form partial monolayers in less than a minute (Fig. 10a) rather than forming lamellar structures. The monolayer coverage is close to that expected if all of the layers seen in the lamellar film were to be consolidated into a single layer (80-90% coverage is the maximum seen to date). Increasing the time or temperature of the heat treatment does not change the size or shape of the monolayer domains. However, above 300°C, small pores nucleate and grow within the domains, and the surface coverage of FDTs drops (Fig. 10b). It appears that the FDTs evaporates from films exposed to temperatures above 300 °C. The ease with which the lamellar-to-monolayer transition and high temperature evaporation occur suggests that FDTs molecules are free to move relative to each other, at least in the early stages of heating. For films processed in isooctane, the ease of structural changes suggest that FDTs molecules deposited at room temperature interact with each other and with the surface primarily via hydrogen bonding rather than by forming a highly crosslinked network of Si-O-Si bonds via condensation. This behavior is consistent with the NMR results suggesting that condensation is slow to negligible in isooctane solutions. Heat treatments can promote the condensation reaction and lock the films into place. For thick films initially containing multilayers of micelles, AFM images show that lamellar structures and even spheres can be retained after high temperature RTP treatments. AFM images have been obtained for a few samples whose structures have been “frozen” via condensation as the spherical phase is in the process of

transforming into the lamellar phase (Fig. 11). Note that lamellar structures appear to be growing from the edges of the spheres, which are now “brittle” in appearance. These RTP results indicate that heat treatment conditions must be selected with care to obtain desired surface morphologies.

## **Discussion**

### Structures of FTDS Agglomerates

Our results indicate that the FDTs spheres seen in the AFM images are the same objects seen in solution via light scattering based on their size and nucleation and growth kinetics. However, it is still not completely clear what the spheres are. The simplest spherical object to consider is an inverse micelle<sup>25</sup> (Fig. 12a). Inverse micelles form when surfactants with hydrophilic head groups and hydrophobic tails are present in hydrophobic organic solvents with a low water content at concentrations exceeding the critical micelle concentration. The hydrocarbon tails on the micelle exterior interact with the solvent, while the hydrophilic head groups line the interior and interact with an encapsulated water droplet. While the shape and nucleation behavior of the objects is consistent with inverse micelles, the size of the objects is too large to be consistent with the NMR results. If all of the water left in a typical isooctane coating solution were encapsulated by all of the hydrolyzed FDTs, the molar ratio of 9 H<sub>2</sub>O:1 hydrolyzed FDTs indicated by the NMR results is consistent with an average micelle diameter of 7.4 nm (forty times smaller than the observed diameter of 300 nm).

It is possible that inverse micelles could aggregate to form 300 nm objects as in inverse microemulsions. Research on the behavior of fluorinated surfactants in water suggests that large spherical droplets of surfactant can form via micelle aggregation in a process resembling a liquid-liquid phase separation (Fig. 12b). However, the driving force for such a phase separation should be less pronounced in isooctane than it is in water. The next simplest circular object to consider is an inverse vesicle (Fig. 12c) consisting of a surfactant bilayer with the head groups and a thin water layer in the layer interior. Isooctane is present both inside and outside the vesicle, whose interior and exterior walls are lined with hydrocarbon chains. In this structure, the vesicle size is independent of the H<sub>2</sub>O:hydrolyzed FDTs ratio. Although the vesicle size cannot be predicted based on solution chemistry, inverse vesicles as large or larger than the objects seen here have been reported for surfactants dissolved in oil.<sup>26</sup> Objects containing nested bilayers (Fig. 12d) (resembling an onion in cross-section) have also been reported.<sup>27</sup>

The AFM results obtained on films heated to 150°C (Fig. 8) are most consistent with a transformation involving the rupture of inverse vesicle structures. After vesicle rupture and solvent evaporation, the skin of the vesicle might lie flat on the surface to form a largely bilayer structure whose lateral dimensions would be about twice that of the parent vesicle. However, the AFM results obtained on “transforming” films (Fig. 11) appear to be more consistent with an inverse micelle aggregate structure for the spheres. On the surface, the aggregates could spread out to form droplets that are 2-3 micelles thick. Removal of the water could transform each micelle layer into a monolayer. Such a transformation would be expected to start on the edges of the spheres as observed rather than being an “explosive” event such as the rupture of a vesicle.

Regardless of which structures are actually present, the light scattering and AFM results indicate that FTDS is capable of organizing into a wide range of aggregate structures similar to those seen for surfactants.<sup>25</sup> In a typical surfactant phase diagram, the dominant phase is controlled by the concentrations of both the surfactant and water in a given solvent. The phase diagram will be different depending on the specific coupling agent, solvent, and reaction temperature used. Such parameters control the extent to which the head groups and tails interact with each other and whether components are locked into place via condensation reactions. A further complication associated with solutions of silane coupling agents is that one of the active components in the diagram, the hydroxylated coupling agent, is being created as a function of time, while another component (the water) is being consumed. This means that the phases present in solution are expected to evolve with time. Finally, a modified diagram will be required to describe the phases present on the substrate surface, as interactions between the hydroxylated head group and the substrate must be included in addition to the interactions involving head groups, tails, and solvent in the bulk solution. Given the range of structures that can form in solution and on surfaces, it is no wonder that researchers have had difficulty in defining appropriate processing conditions for producing monolayers in a reproducible fashion. It is also no surprise that different groups obtain different results with different combinations of solvents, solvent water contents, and coupling agents. While it was beyond the scope of this project to determine phase diagrams for FDTs-water-solvent systems, it appears that spherical agglomerates are the dominant structures present in all solvents and at all water contents investigated once FTDS hydrolysis has occurred. For films deposited at room temperature, spherical agglomerates or monolayers are always



seen. The lamellar phase has only been observed for samples which have seen a sufficient heat treatment to remove the bulk of the solvent and the water.

### Processing and Performance Implications

Given the complexities associated with FTDS deposition solutions, it is important to establish guidelines that can be used to favor the formation of the desired self-assembled monolayers. The simplest method for obtaining a monolayer is to use fresh deposition solutions in which the concentration of the hydroxylated coupling agent has not yet reached the critical aggregation concentration. The induction time for aggregate formation depends on the coupling agent, the solvent, and the solvent water content. For FDTS in isooctane, induction times range from a few minutes to over two hours depending on whether the solvent is saturated with water (at 2.3 mM) or dry (< 0.2 mM). Previous studies have shown that pretreatment of Si substrates can improve coating reproducibility by promoting hydrolysis on the surface. Use of a “wet” substrate in a “dry” solvent is expected to yield the best results. However, water layers on “wet” substrates will dissolve in “dry” solvents, decreasing the surface water content and increasing the solvent water content until solution water concentrations reach the solubility limit. Care must be taken to keep processing times relatively short and to not try to coat too many substrates in the same coating solution. For 1 mM FTDS in isooctane, we recommend starting with dry solvent (< 0.2 mM), using dry containers and fixtures, coating no more than twenty 4” wafers per 100 ml of coating solution, and removing all substrates from the solution in less than one hour after the initial FDTS addition. (This will normally limit the use of the coating solution to one batch of wafers.)

Although extensive studies were not performed to determine the role of solvent and coupling agent on self-organization in solution, some trends can be predicted based on the limited NMR observations to date. At least for short chain coupling agents, the critical aggregation concentration tends to be higher in solvents that are more polar. This is because the hydroxylated head groups have a higher effective solubility in polar solvents. Trends in critical micelle concentration (cmc) should mirror the solubility of water in a given solvent ( $\text{CHCl}_3 > \text{toluene} > \text{CCl}_4 > \text{isooctane}$ ). However, unless care is taken to dry the solvents, more water will be present in solvents having a high cmc. In addition, at identical water contents, hydrolysis and condensation rates are faster in more polar solvents. This means that although the cmc is higher for  $\text{CHCl}_3$  than it is in isooctane, the cmc may be reached sooner in  $\text{CHCl}_3$  if the  $\text{CHCl}_3$  is wet. On the other hand, if the  $\text{CHCl}_3$  is scrupulously dried, it will be more effective at dissolving the thin water layer present on substrate surfaces, which may inhibit monolayer formation.

Predicting the effect of the coupling agent on the processing window available for monolayer formation is also complex. In general, it appears that better results are obtained when the driving force for self assembly in solution is driven more by the chains than by the hydrolyzed head group. Monolayer formation appears to be favored by increasing the chain length. (This is why ODTs precipitated in water assumes a lamellar rather than an inverse micelle structure.<sup>24</sup>) Aggregation of the head groups can be suppressed by replacing one or two of the chloro- groups with methyl groups. Unfortunately, the presence of methyl groups can sterically interfere with monolayer formation, inhibiting the kinetics of film formation and producing films with low packing densities.<sup>28</sup> Chain solvation is clearly important, and may contribute to the fact that 1

mM solutions of fluorinated coupling agents such as FDTS are more prone to aggregate in solution than comparable ODTs solutions even though both systems have comparable transition temperatures for chain ordering.

After deposition, changes in either temperature or humidity can influence the distribution of phases on the substrate. The AFM images presented here indicate that removal of water promotes transitions from droplets to lamellar structures to monolayers. Conversely, previous work has shown that exposing monolayers to humid environments can lead to a restructuring to form spherical objects resembling those shown here.<sup>6</sup> At a minimum, restructuring of a monolayer will reduce the surface coverage of coupling agent, creating bare patches. Depending on what structures form, the surface can also end up being terminated by silanol groups rather than hydrocarbon chain. Both factors can lead to a deterioration of the anti-stiction or anti-friction properties of the film. Thermal treatments that promote condensation reactions between silanol groups can lock surface structures into place, inhibiting surface reorganization. However, care must be taken to ensure that mild heating is performed to remove water and promote monolayer formation before the high-temperature cure to remove silanols is performed.

In summary, the aggregation of hydrolyzed silane coupling agents in solution can impact the quality of self-assembled monolayers. Irreproducible results in coating quality can often be attributed to whether or not aggregates are formed during the time interval in which substrates are exposed to the coating solution. (Beam release experiments performed on micromachined parts to monitor stiction indicate that release occurs for samples in which simple monolayers are present, while release is inhibited when FTDS aggregates are observed.) Factors that influence the induction time for aggregate

formation include the solvent, its water content, and coupling agent concentrations. The time window available for producing quality coatings from a given coating solution can be maximized by scrupulously drying solvents prior to FDTS addition. Processing times can also be manipulated and controlled if the phase behavior of the coupling agent-water-solvent phase diagram is known. For thin coatings, heat treatments can sometimes restructure surface aggregates into lamellar or monolayer structures. Such heat treatments also promote condensation reactions that tend to lock film structures into place. A two-step heating procedure is recommended if monolayer formation is desired (heating at 100-150°C to promote film restructuring, followed by a short treatment at 250-300°C to promote condensation and cross-linking). The crosslinking step should also enhance long-term film stability.

**Acknowledgement.** The authors would like to thank Peggy Clews for providing the motivation for the project and for her insights regarding the processing of self-assembled monolayers in a production setting. R.W.C. acknowledges the support of the Natural Sciences and Engineering Research Council of Canada. The work was supported by Laboratory Directed Research and Development funds at Sandia National Laboratories. Sandia is a multiprogram laboratory operated by Sandia Corporation, a Lockheed Martin Company, for the United States Department of Energy under Contract DE-ACO4-94AL85000.

## References

1. Maboudian, R.; Howe, R. T. *J. Vac. Sci. Technol. B* **1997**, 15, 1
2. Brzoska, J. B.; Azouz, I. B.; Rondelez, F. *Langmuir* **1994**, 10, 4367
3. Parikh, A. N.; Allara, D. L.; Azouz, I. B.; Rondelez, F. *J. Phys. Chem.* **1994**, 98, 7577
4. McGovern, M. E.; Kallury, M. R.; Thompson, M. *Langmuir* **1994**, 10, 3607
5. Le Grange, J. D.; Markham, J. L.; Kurkjian, C. R. *Langmuir* **1993**, 9, 1749
6. de Boer, M. P.; Mayer, T. M.; Michalske, T. A.; Srinivasan, U.; Maboudian, R.
7. Sagiv, J. *J. Am. Chem. Soc.* **1980**, 102, 92
8. Pribakar, S.; Assink, R. A.; Raman, N. K.; Myers, S. A.; Brinker, C. J. *J. Non-Cryst. Solids* **1996**, 202, 53
9. Feng, X.; Fryxell, G. E.; Wang, L.-Q.; Kim, A. Y.; Liu, J.; Kemner, K. M. *Science* **1997**, 276, 923
10. Tripp, C. P.; Hair, M. L. *Langmuir* **1995**, 11, 1215

11. Carraro, C.; Yauw, O. W.; Sung, M. M.; Maboudian, R. *J. Phys. Chem. B.* **1998**, 102, 4441
12. Srinivasan, U.; Houston, M. R.; Howe, R. T.; Maboudian, R.
13. Martin, J. E.; Wilcoxon, J. P.; Schaefer, D.; Odinek, J. *Phys. Rev. A*, **1990**, 41, 4379
14. Sindorf, D. W.; Maciel, G. E. *J. Am. Chem. Soc.* **1983**, 105, 3767
15. Guo, W.; Brown, T. A.; Fung, B. M. *J. Phys. Chem.* **1991**, 95 1829
16. Kinrade, S. D. *J. Phys. Chem.* **1996**, 100, 4760
17. Baney, R. H.; Itoh, M.; Sakakibara, A.; Suzuki, T. *Chem. Rev.* **1995**, 95, 1409
18. Martin, J. E.; Wilcoxon, J.; Adolf, D. *Phys. Rev. A*, 1987, 36, 1803
19. Israelachvili, J.; *Intermolecular and Surface Forces*; Academic Press: San Diego, 1992
20. Drelich, J.; Wilbur, J. L.; Miller, J. D.; Whitesides, G. M. *Langmuir* **1996**, 12, 1913
21. Onda, T.; Shibuichi, S.; Satoh, N.; Tsujii, K. *Langmuir* **1996**, 12, 2125

22. Brzoska, J. B.; Azouz, I. B.; Rondelez, F. *Langmuir* **1994**, *10*, 4367
23. Rye, R. R. *Langmuir* **1997**, *13*, 2588
24. Parikh, A. N.; Schivley, M. A.; Koo, E.; Sheshadri, K.; Aurentz, D. Mueller, K.; Allara, D. L. *J. Am. Chem. Soc.* **1997**, *119*, 3135
25. Tiddy, G. J. T. *Phys. Reports* **1980**, *57*, 1
26. Kunieda, H.; Nakamura, K; Davis, H. T.; Evans, D. F. *Langmuir*, **1991**, *7*, 1915
27. Lu, Y.; Fan, H.; Stump, A.; Ward, T. L.; Rieker, T.; Brinker, C. J. *Nature* **1999**, *398*, 223
28. Rye, R. R.; Nelson, G. C.; Dugger, M. T. *Langmuir* **1997**, *13*, 2965

### Figure Captions

Figure 1. Schematic diagram illustrating reactions leading to the deposition of coupling reactions on wet Si substrates.

Figure 2.  $^{17}\text{O}$  NMR spectra vs. time for 8 mM solution in FDTS and water in  $\text{CCl}_4$ .

Figure 3. Relative species concentrations vs. time in FDTS coating solutions based on  $^{17}\text{O}$  NMR peak intensities: a) in 1 mM FDTS + 2.3 mM water in isooctane, and b) in a  $\text{CCl}_4$  solution that is 8 mM in both FTDS and water.

Figure 4.  $^{17}\text{O}$  NMR spectra vs. time for a 17 mM solution of both FDTS and water in  $\text{CHCl}_3$ .

Figure 5. a) Scattered light intensity vs. time and water content for FDTS solutions in isooctane; b) Average hydrodynamic radius of objects in the same FDTS solutions vs. time and water content.

Figure 6. Contact angles for water on FDTS coated Si substrates vs. coating time and water content of 1 mM FDTS coating solutions in wet (w) and dry (d) isooctane, wet isooctane containing 10 vol% isopropanol (I), and wet  $\text{CCl}_4$  (C).

Figure 7. a) Tapping mode AFM image (size =  $5\ \mu\text{m} \times 5\ \mu\text{m}$ ) of Si wafer after immersion in FDTS-isooctane solution for times exceeding the induction time for solution aggregation; b) Line scan in AFM image across circular object indicated in Fig. 8a.



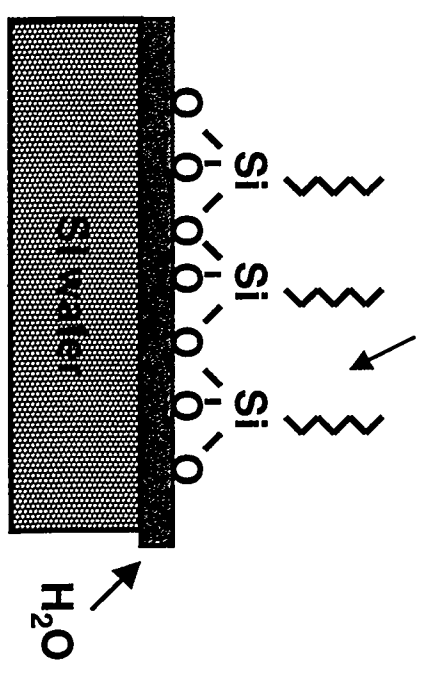
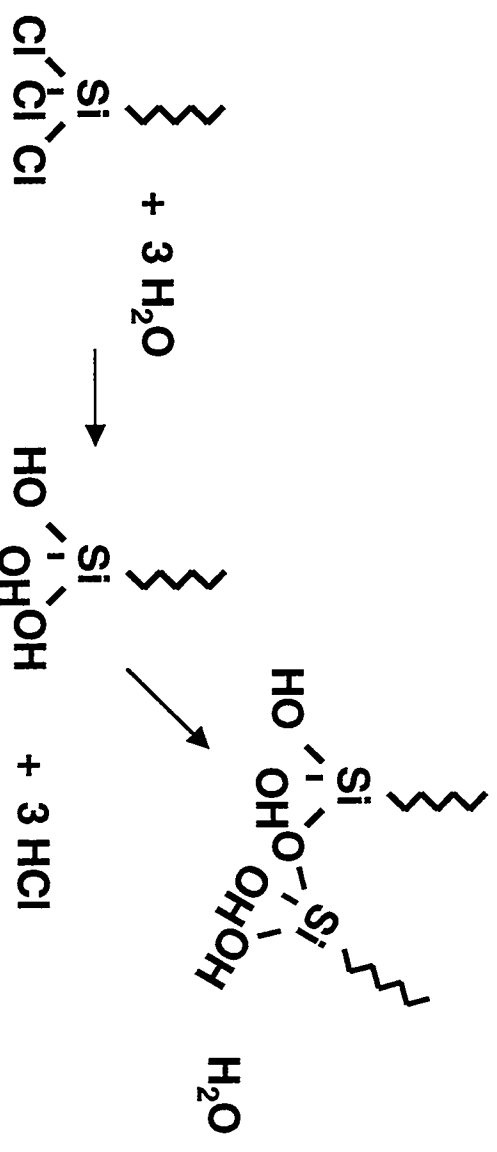
Figure 8. a) Tapping mode AFM image ( $2\ \mu\text{m} \times 2\ \mu\text{m}$ ) of FDTs-coated Si wafer after RTP heat treatment at  $150^\circ\text{C}$  for one minute. Prior to heat treatment, the sample morphology was similar to the sample depicted in Fig. 7a; b) Line scan in AFM image of object shown by line in Fig. 8a. showing discrete steps equivalent to one chain length.

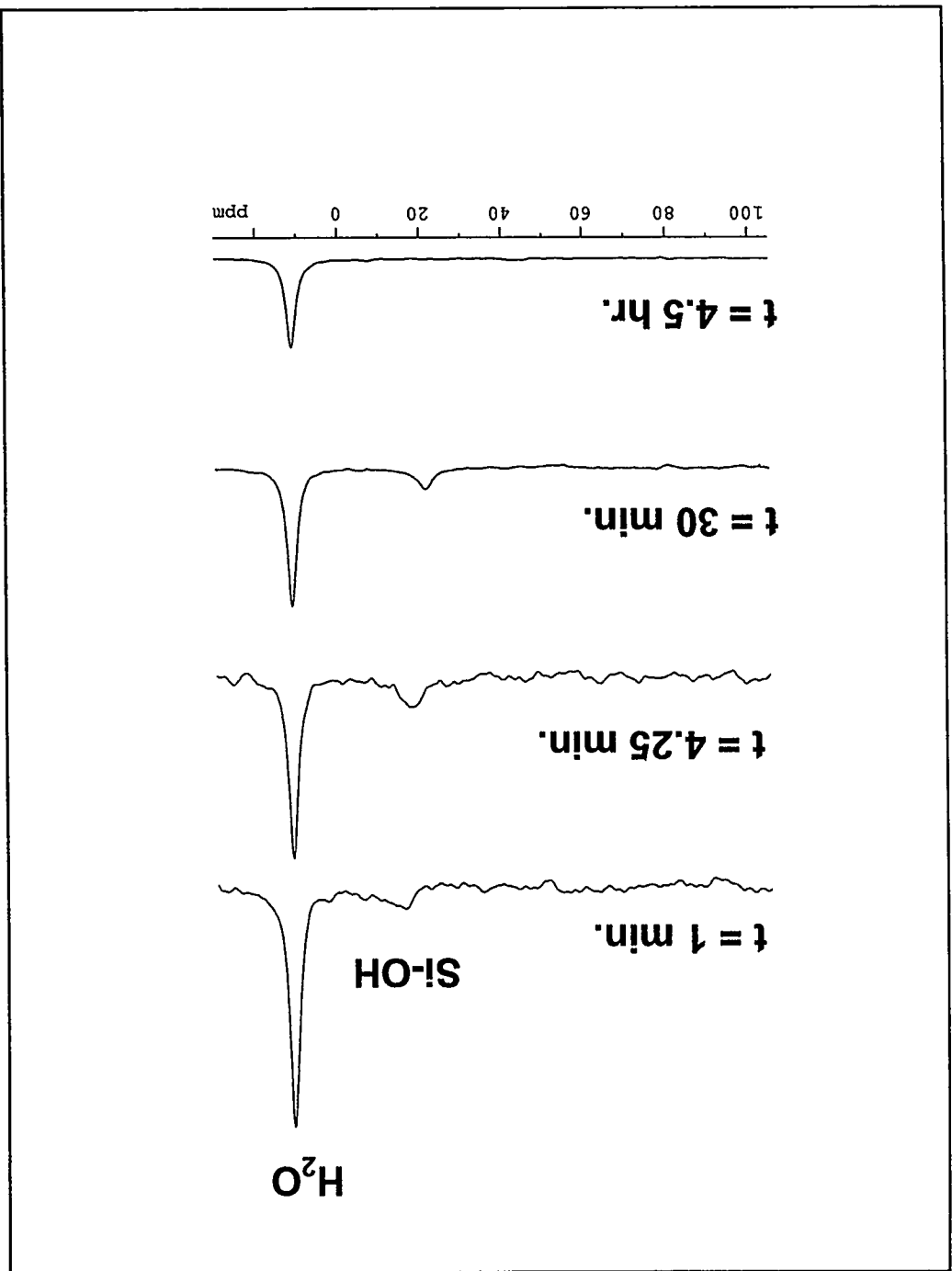
Figure 9. a) Contact mode AFM friction image ( $2\ \mu\text{m} \times 2\ \mu\text{m}$ ) of lamellar structure similar to that shown in the tapping mode image in Fig. 8a; b) Friction image corresponding to the contact mode image shown in Fig. 9a; c) Depiction of lamellar structure that would generate contrast between high and low friction between layers.

Figure 10. a) Tapping mode AFM image ( $10\ \mu\text{m} \times 10\ \mu\text{m}$ ) of monolayer formed on FDTs-coated Si wafer after RTP heat treatment of  $250^\circ\text{C}$  for 5 minutes; b) Tapping mode AFM image ( $2\ \mu\text{m} \times 2\ \mu\text{m}$ ) of FDTs-coated Si wafer after heat treatment at  $350^\circ\text{C}$  for 5 minutes showing the appearance of porosity within the monolayer islands.

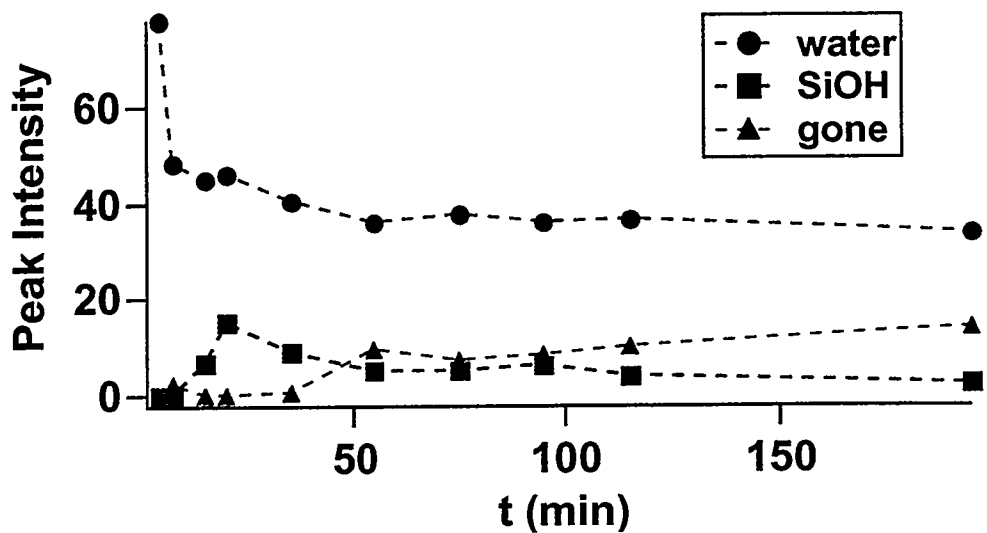
Figure 11. Tapping mode AFM image ( $1\ \mu\text{m} \times 1\ \mu\text{m}$ ) showing the transformation of spherical deposits into lamellar deposits.

Figure 12. Representations of possible aggregate structures: a) inverse micelles, b) micelle aggregates, c) inverse vesicles, d) nested vesicles.

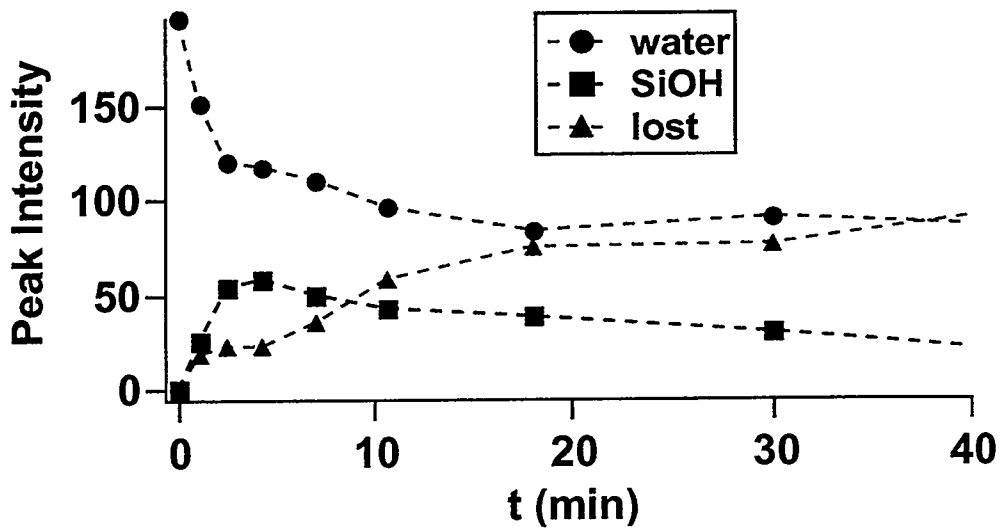


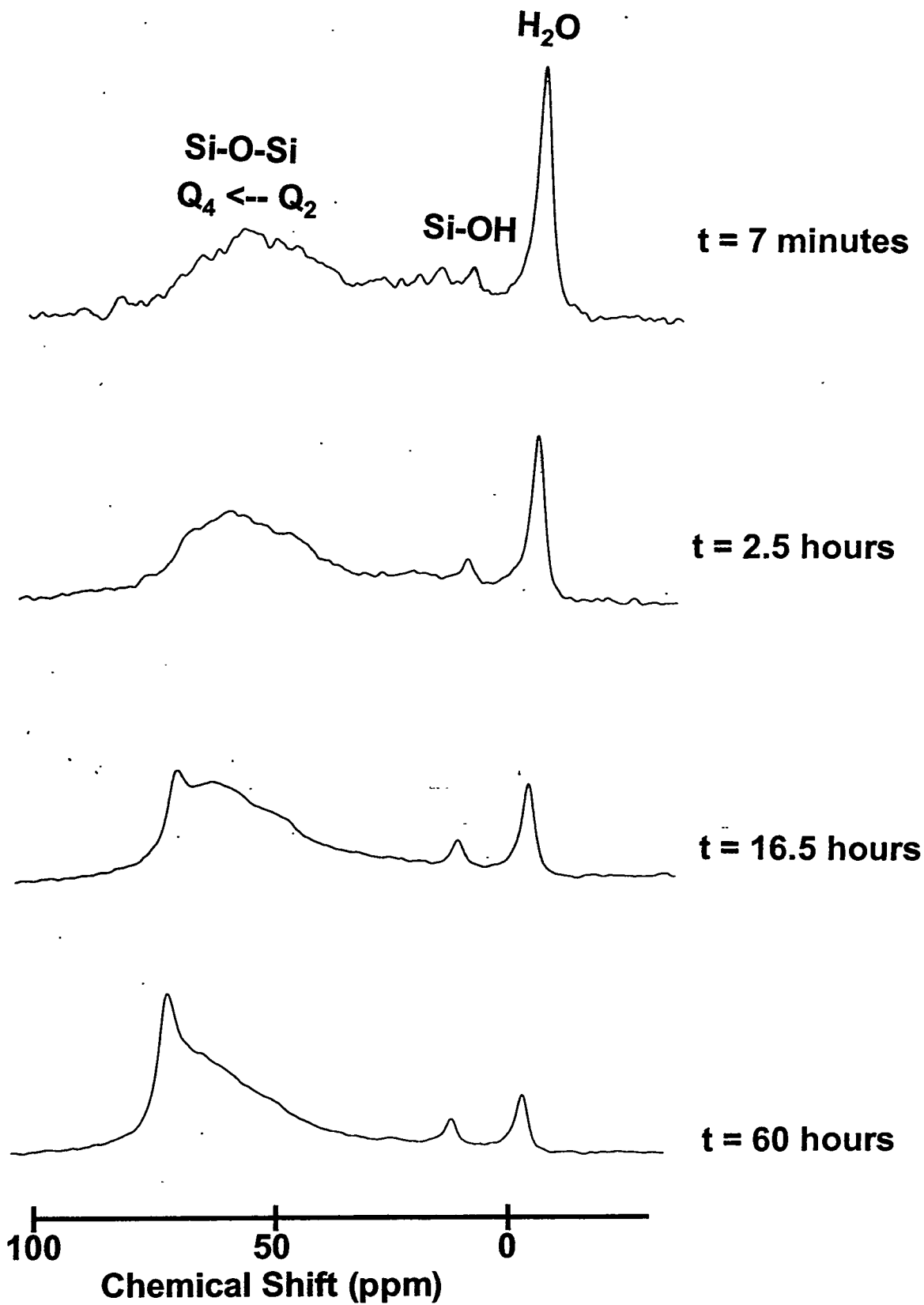


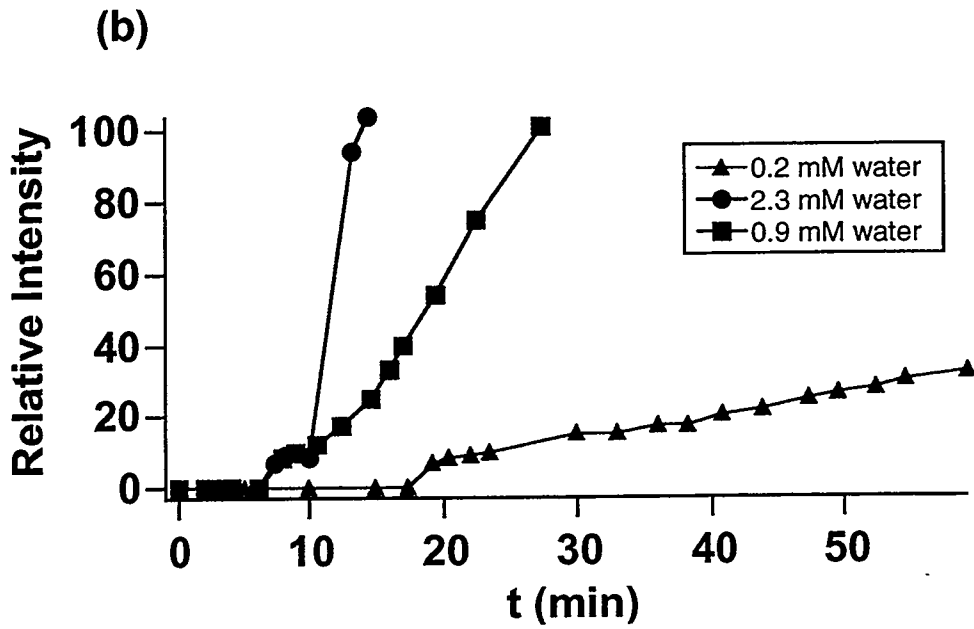
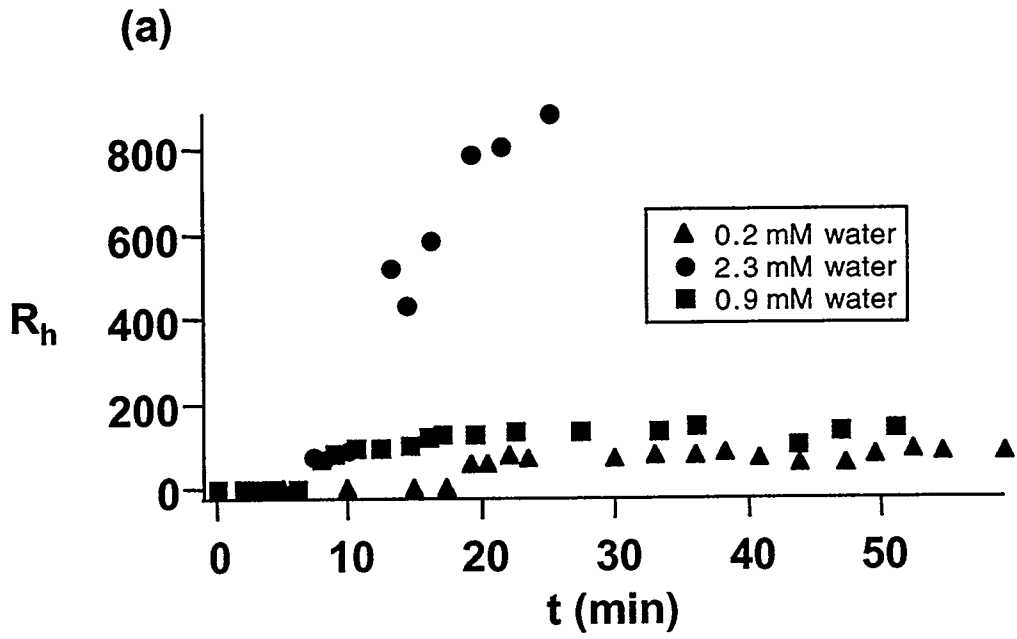
(a) 1 mM FTDS + 2.3 mM H<sub>2</sub>O  
in isooctane

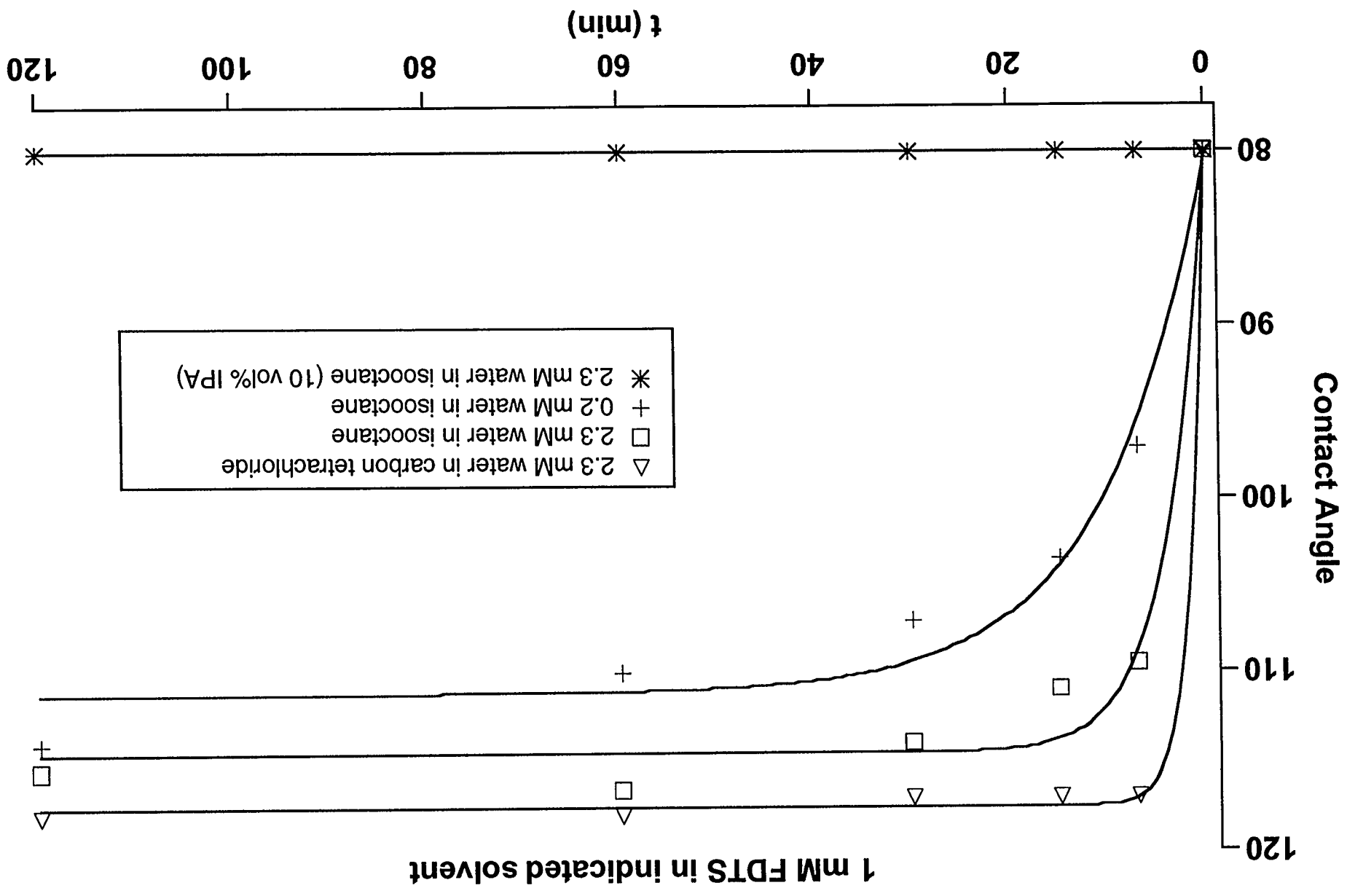


(b) 8 mM FTDS + 8 mM H<sub>2</sub>O  
in CCl<sub>4</sub>

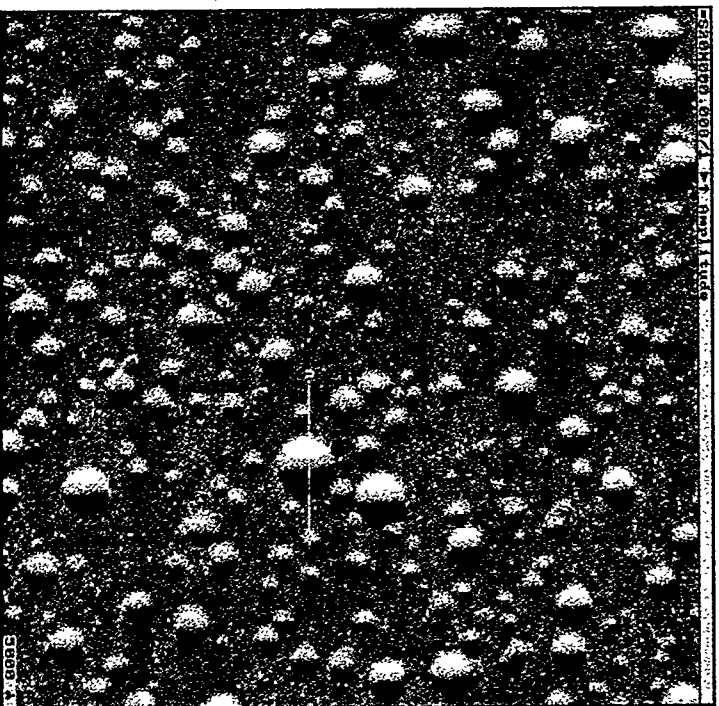




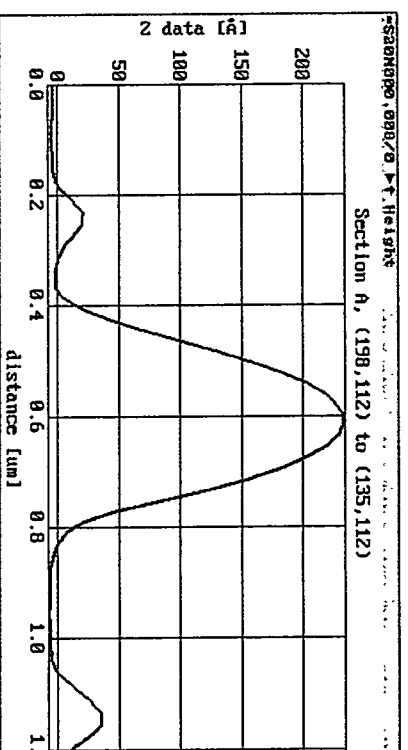




**(a) Tapping Mode AFM Image**

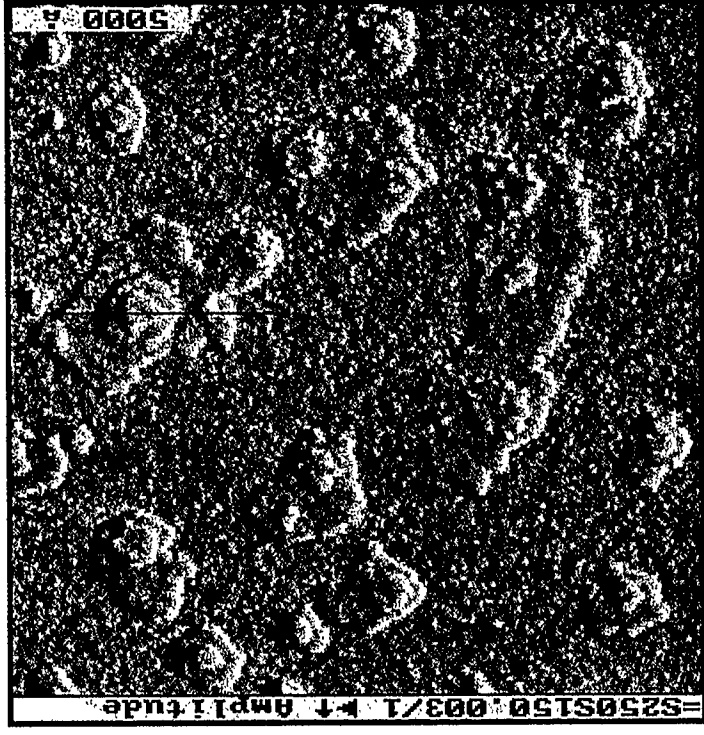


**(b) AFM Line Scan**



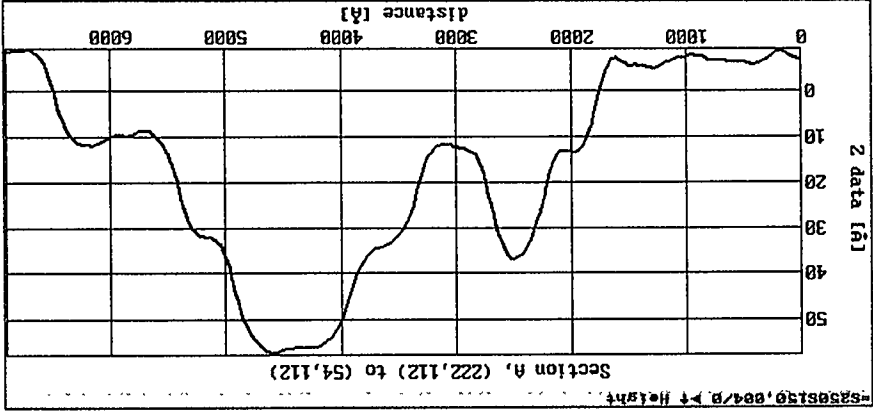
**1 mM FTDS + 10 ppm H<sub>2</sub>O in isooctane  
Deposition time = 1 hour**





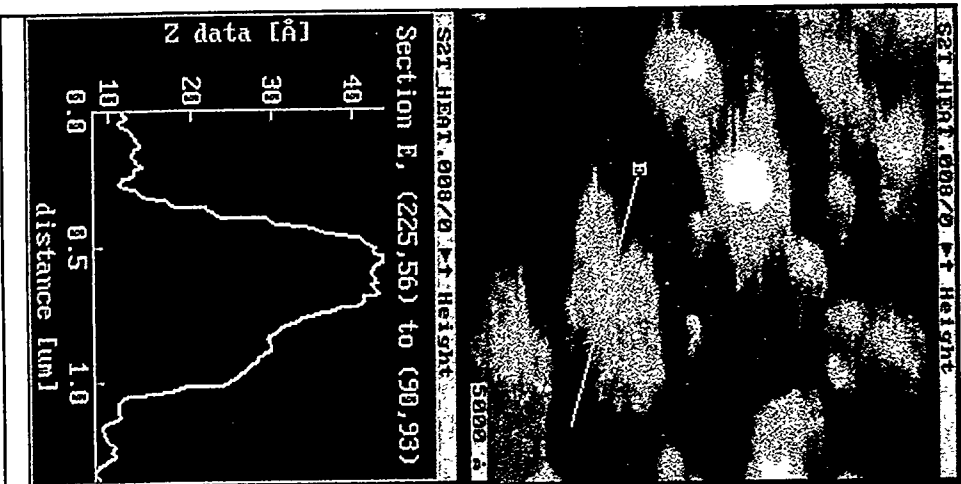
(a) tapping mode image

1 mM FDS + 10 ppm water  
 in isooctane  
 deposition time = 1 hour  
 RTP temperature = 150°C  
 RTP time = 50 seconds

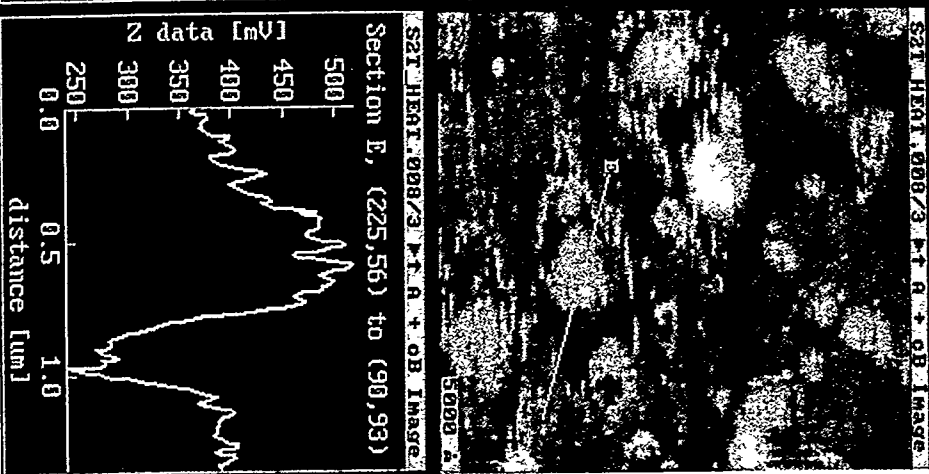


(b) line scan

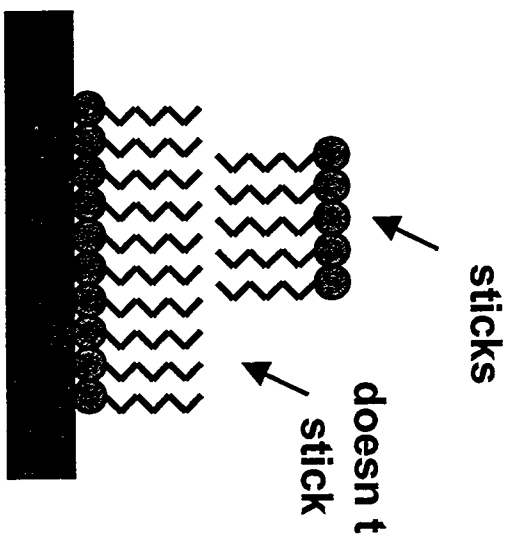
a) contact mode image



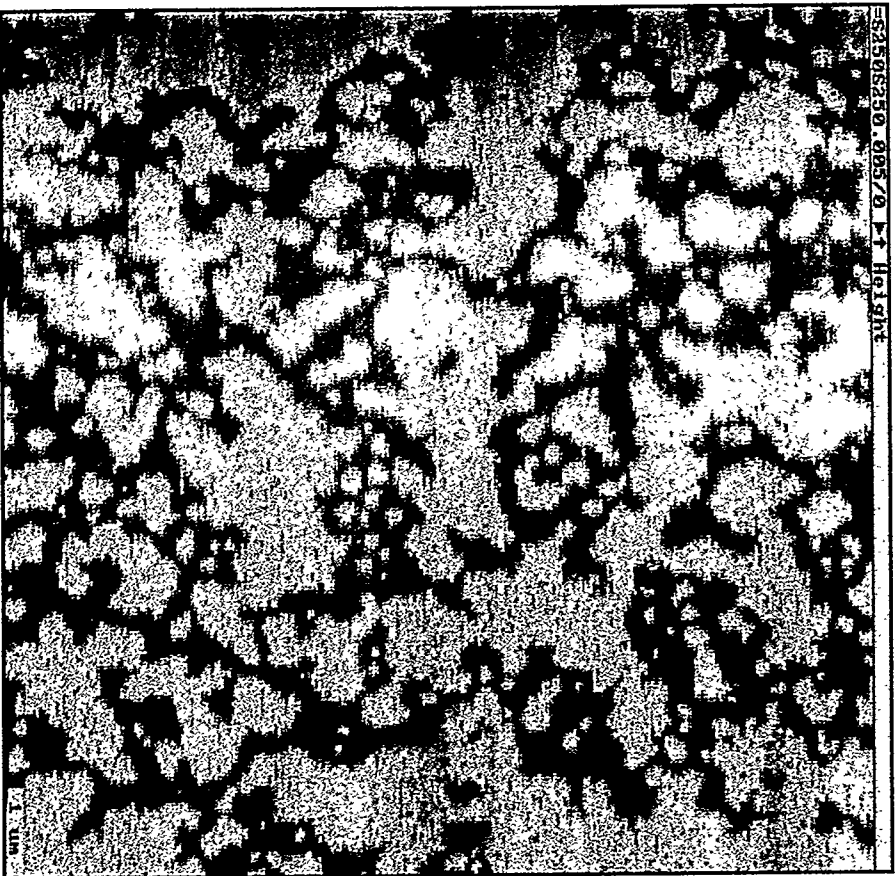
b) friction image



c) proposed lamellar structure

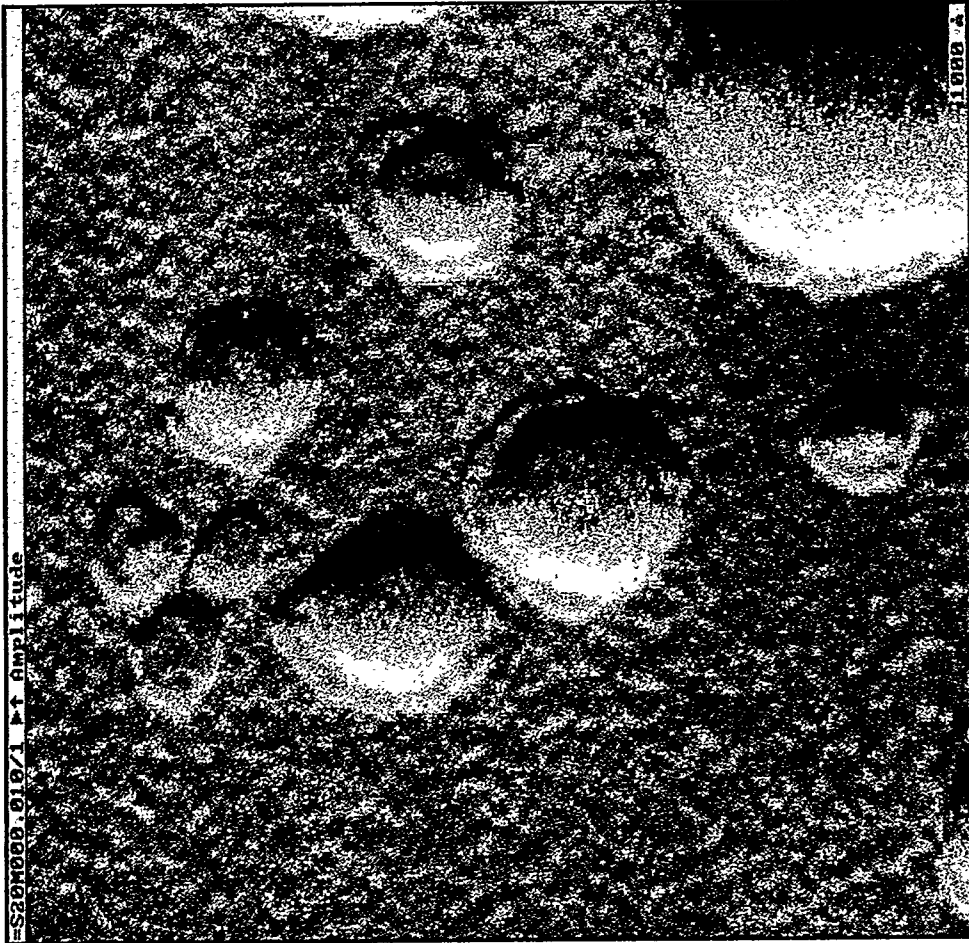


**(a) monolayer film after 250°C, 5 min.**

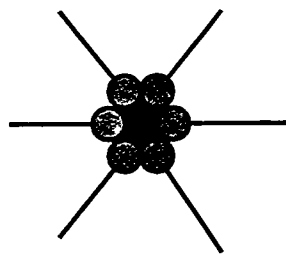


**(b) porous monolayer after 350°C, 5 min.**

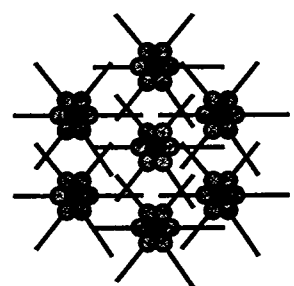




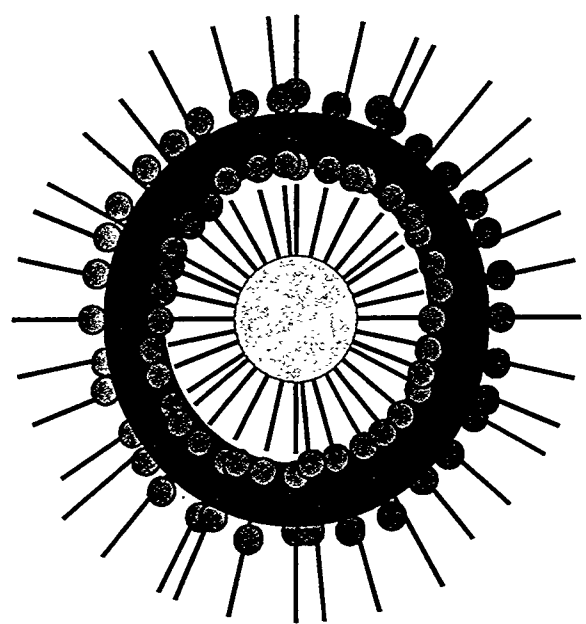
(a)



(b)



(c)



(d)

